Iranian Journal of Materials Science and Engineering, Vol. 19, Number 3, September 2022
RESEARCH PAPER

Effects of Al Doping on the Properties of $Li_7La_3Zr_2O_{12}$ Garnet Solid Electrolyte Synthesized by Combustion Sol-Gel Method

Omid Sharifi[1], Mohammad Golmohammad[1,*], Mozhdeh Soozandeh[1], Mohammad Oskouee[2]

* *mgolmohammad@nri.ac.ir*

[1] Renewable Energy Department, Niroo Research Institute (NRI), Tehran, Iran
[2] EV Development Center, Niroo Research Institute (NRI), Tehran, Iran

Received: January 2022 **Revised: February 2022** **Accepted: March 2022**

DOI: 10.22068/ijmse.2631

Abstract: *$Li_7La_3Zr_2O_{12}$ (LLZO) garnets are considered as promising materials for electrolytes in solid-state batteries. In this study, $Li_{7-3x}Al_xLa_3Zr_2O_{12}$ (x= 0.22, 0.25, and 0.28) garnet was synthesized using the combustion sol-gel method to stabilize the cubic phase for higher ionic conductivity. The X-ray diffraction (XRD) results of as-synthesized powders revealed that by addition of 0.22 and 0.25 mole Al, the tetragonal persists to exist, whereas 0.28 mole Al addition resulted in a single cubic phase. Afterward, the as-synthesized powders were pressed and sintered at 1180°C for 10h. The hardness evaluation revealed that Al addition increased the hardness that caused better resistance against Li dendrite formation. The secondary electron microscopy results demonstrated that the dopant did not have a huge impact on particle size and grain growth. However, the porosity content was changed. Finally, electrochemical behaviour studies showed that, the addition of Al increased the ionic conductivity of samples by increasing the density and stability of the cubic phase. The results indicated that the sample containing 0.25 mole Al sample had the highest ionic conductivity. This behaviour is believed to be the result of the promotion of sintering and an increase in the bulk ionic conductivity by Al doping.*

Keywords: *Solid electrolyte, Combustion sol-gel, Electrochemical characteristics, $Li_7La_3Zr_2O_{12}$ (LLZO), Al-doped.*

1. INTRODUCTION

Lithium-ion batteries have attracted a lot of attention due to their higher energy and power density [1-4]. Nowadays, solid-state batteries have played essential roles as energy storage devices [5-7]. Also, compared to liquid electrolytes, solid electrolyte technology is currently promising to be used in devices, especially electric vehicles and energy storage devices, because of their higher safety, the potential for longer life, and higher capacity.

Different types of solid electrolytes have been introduced, such as garnet [8-10], perovskite [8, 11], Nasicon [8, 11], Lisicon [8, 12], etc. Despite the old history of solid electrolytes, in 2007, Murugan and Weppner reported garnet-type solid electrolytes with high ionic conductivity for the first time. These garnet electrolytes showed promising behavior due to high stability against Li electrodes, competent ionic conductivity, and reliable thermal stability. Although, the cubic crystalline phase of LLZO revealed the competent ionic conductivity (about 10^{-4} S cm^{-1}), whereas the tetragonal phase (the other stable crystalline phase) is two times the magnitude lower in conductivity (about 10^{-6} S cm^{-1}) [7].

Stabilizing the cubic phase is a challenge, and different efforts are performed to overcome this hurdle. One of the main solutions is using dopants to stabilize the cubic phase. Different dopants such as Al [13-17], Ga [18-21], Nb [22, 23], Ta [24-26], etc., have been used to stabilize the LLZO cubic phase by creating vacancies and increasing irregularities while increasing ionic conductivity. Among these dopants, Al has received a lot of attention due to its cost-effectiveness and improving the sintering process. It is worth mentioning that different amounts of Al between 0.2 and 0.3 have been proposed for the optimum amounts.

Despite the dopant, the synthesis method impacts phase evolution and the final ionic conductivity of the sample. For instance, Matsuda et al.'s results showed only the tetragonal phase by adding 0.2 moles Al by the solid-state method [27], whereas Rangasami et al. synthesized the cubic phase with 0.2 moles Al, by the sol-gel method [28]. This indicates that the synthesis method, in addition to substitution, can affect the stabilization of the cubic phase. Different types of synthesis methods such as sol-gel [29-33], solid-state [6, 18, 34, 35], solution-based [36, 37], etc., have been used to synthesize LLZO. Amongst all of these methods,

[DOI: 10.22068/ijmse.2631]

solid-state and sol-gel attracted more attention. The solid-state process is the simplest, although, higher calcination temperature and longer time resulted in a lithium deficiency in synthesized powder.

On the other hand, the sol-gel method has several advantages, such as shorter time and lower temperature of calcination, while the controlling stoichiometry is simpler [38-40]. Among different sol-gel methods type, the combustion sol-gel method has been deserted, and there are not many reports on that. Moreover, the cubic phase is obtained in a broader range of lithium concentrations by the sol-gel method.

The combustion sol-gel method is a time-saving method with excellent stoichiometric control and homogeneity of the resulting materials, which discrete it from other synthesis methods. In the combustion sol-gel method, the materials are mixed in a solution, which helps to react better with each other. Generally, using the combustion sol-gel method can improve lithium deficiency by lowering the time and temperature that powders were subjected to and also increasing the share of cubic phase as the nature of the synthesis method [16, 29, 38, 41].

As it was mentioned, different amounts of Al were proposed as the optimum content. In our previous work, three amounts of Al (0.2, 0.25, and 0.3 mol) as dopant were studied and the optimum amount was obtained 0.25 mol. Although, some other researches [14, 17, 23] reported different optimum amounts. Therefore, in this study, the effects of different Al concentrations (0.22, 0.25, and 0.28) on the properties of LLZO were investigated to produce a stabilized cubic phase with a high Li-ion conductivity electrolyte. To achieve that, we investigated the effect of Al content on phase and microstructure evolution of as-synthesized powder and sintered pellets. Finally, the electrochemical behaviors of sintered samples were studied using the electrochemical impedance spectroscopy (EIS) technique.

2. EXPERIMENTAL PROCEDURE

2.1. Materials

$Li_{7-3x}Al_xLa_3Zr_2O_{12}$ (x= 0, 0.22, 0.25, 0.28) garnet powder were synthesized in a 5g batches, using combustion sol-gel method. Stoichiometric amounts of high purity $Al(NO_3)_3$ (Merck, >98.5%), $La(NO_3)_3$ (Sigma-Aldrich, 99%), $Zr(C_5H_7O_2)_4$ (Merck, >99%), and $LiNO_3$ (Merck, >98%) (and 10% moles excess of Li to avoid the loss of lithium during calcination) and $CO(NH_2)_2$(Merck, >99%) were solved in deionized water and were stirred at 300°C. The $CO(NH_2)_2$ (urea) were added as the fuel source with the stoichiometric amount to the sum of reduction and oxidation agents. It was continued until the water was vaporized and a white gel was obtained. The gel was dried at 120°C for 6 h and then calcined at 1000°C for 1 hour in the air [16]. The as-synthesized powders with 5% of the binder (PVB[1]) were uniaxially pressed (100 MPa pressure) into the pellets with a diameter of 15mm, afterward, pellets were sintered at 1180°C for 10 hours. The pellets were embedded with the same mother powder in the alumina Crucible, to avoid lithium loss. Moreover, the sample was quenched from high temperature to avoid degradation of sample due to formation of LiOH and/or $LiCO_3$.

2.2. Characterization

X-ray diffraction (XRD, PHILIPS, PW1730) with Cu k_α radiation (λ= 1.5418 Å) were performed over an angular range of 20-60° to understand phase evolution. The surface area of obtained powder was analyzed using Brunauer-Emmett-Teller Surface Area & Porosity Analyzer (BET, micromeritics). The microstructure and morphology of samples were characterized by using a field-emission scanning electron microscope (FESEM, TESCAN; Mira3). The densities of sintered pellets were evaluated using the Archimedes method. The hardness of the samples was evaluated using Vickers indenters (ASTM C1327 - 15). The hardnesses were calculated from the ratio of the applied force to the area of contact of the four faces of the undeformed indenter. Finally, before the electrochemical evaluation, the sintered samples were slightly polished. Then Au paste was applied on both sides of pellets for impedance measurements. Electrochemical impedance spectroscopy was applied using a (PotantioStat-Autolab 302N) over the range of 0.1 Hz–100 KHz frequency with an alternating voltage of 10 mV. Measurements were recorded at 30°C in the air.

[1] Polyvinyl butyral

[DOI: 10.22068/ijmse.2631]

3. RESULT AND DISCUSSION

The XRD patterns of $Li_{7-3x}Al_xLa_3Zr_2O_{12}$ (x= 0, 0.22, 0.25, 0.28) is shown in Fig. 1. For the sample without Al dopant, the main phase is tetragonal, whereas, with the addition of Al, the share of the cubic phase increases. Although, the sample with 0.22 and 0.25 moles doped Al, still the tetragonal phase is observable in the powders, whereas for the 0.28 mole doped sample, the tetragonal phase is diminished. No impurity peaks rather than LLZO were seen in the XRD detection range.

This behavior was seen by other researchers that with the increasing amount of Al, more tetragonal peaks transformed into cubic phases. The cubic phase stability of garnet is affected by the concentration of lithium and Al [42, 43]. A single cubic phase is observed, and there is only one additional peak at an angle of 28° when the amount of dopant is increased to 0.25 moles of Al (Fig. 1), which can be attributed to the tetragonal phase. X-ray diffraction pattern of Al-28 (Fig. 1) shows a single cubic phase and does not show any impurities.

Replacing one Al^{3+} with Li^+ generates two Li vacancies increasing the lithium vacancy concentration. It also causes phase transfer from tetragonal to cubic by destabilizing lithium in the tetragonal phase, which also affects the conductivity and mobility of lithium ions [29, 44-46]. Even though the solubility of Al in LLZO structure is presented 0.25 moles by Matsuda et al [27]. Herein, 0.28 mole Al showed no impurities. Besides, Matsuda et al. synthesized a cubic phase with $LaAlO_3$ impurity by the solid-state method with 0.26 mole of dopant, which could be due to less reactivity of raw materials with each other during synthesis according to the manufacturing process. They obtained only the tetragonal phase with 0.2 moles of Al [27].

Rangasami et al. observed that the cubic phase can be stabilized with at least 0.204 moles of Al. Some impurity phases, such as $La_2Zr_2O_7$ was observed in the synthesized powder by the solid-state method [28]. However, in this study, by combustion sol-gel synthesis method with 0.2 moles Al as dopant, no impurity was observed, and the dominant phase was cubic. This can be related to the better reaction of raw materials in solution in the sol-gel method. Compared to the solid-state method, which requires a higher lithium concentration and more energy to achieve the cubic phase, in the sol-gel method, the cubic phase is obtained in a broader range of lithium concentrations [38].

It can be concluded that depending on the different conditions of synthesis, the minimum amount of doped Al to stabilize the cubic phase at room temperature is not a fixed value.

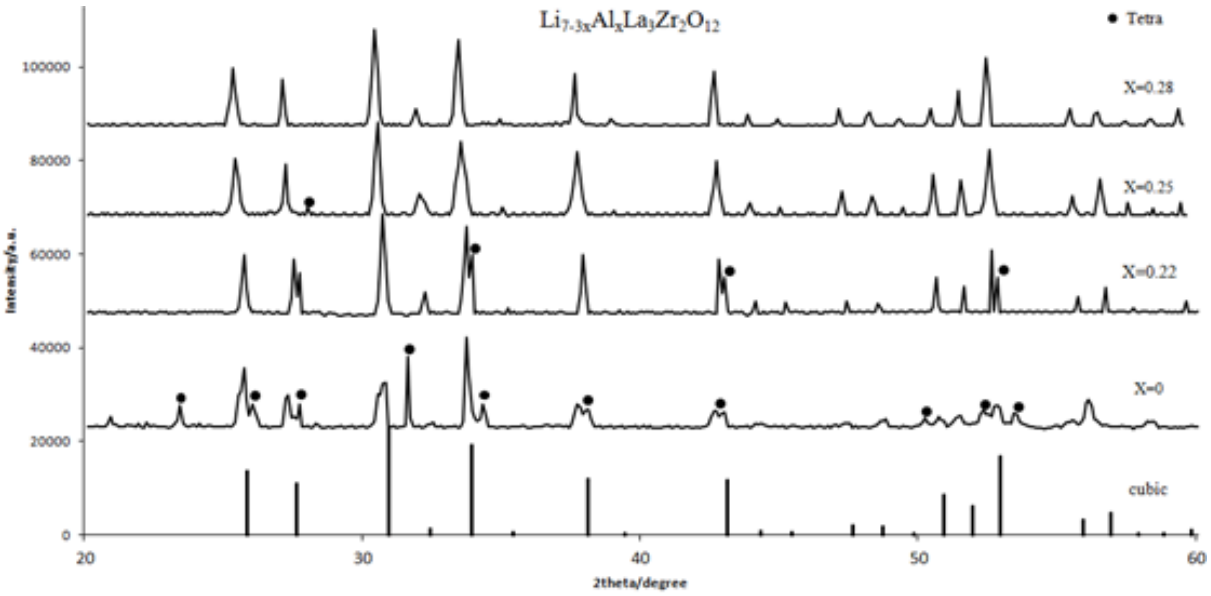

Fig. 1. XRD pattern of Al-doped garnet powder, synthesized at 1000°C for 1 hour.

[DOI: 10.22068/ijmse.2631]

The BET result of the sample revealed that the powders almost have the same surface area as 4.3, 4.2, and 4.2 m^2g^{-1} for 0.22, 0.25, and 0.28 doped samples, respectively. Afterward, the powder was pressed and sintered at 1180 for 10 hours, and the X-ray diffraction pattern is shown in Fig. 2

By matching the PDF card of the cubic and tetragonal phase with the X-ray pattern, it is clear that the main phase is the cubic in garnet with 0.22 mole Al (Al-22). Some of the calcined garnet powder, which remained in the tetragonal phase and had not been transformed to the cubic phase, was completely transformed to the cubic phase during sintering. Also, the cubic phase peaks were seen in the X-ray pattern of Garnet with 0.25 and 0.28 moles of Al doping (Al-25 and Al-28), while no impurity phase was observed. X-ray patterns show that all three samples (Al-22, Al-25, and Al-28) have cubic phases and have no impurity phases. According to previous studies, with increasing sinter temperature from 1130 to 1150°C, the structure changes, and from 1150 to 1230, the cubic phase crystallizes [47]. In this work, we showed that the sol-gel method could be effective in lowering the stabilization temperature of the LLZO cubic phase.

The summary of the results of the density and hardness of the sintered garnet is given in Table 1. Garnet with 0.22 mole Al additives has a relative density of 82.4%, which is not suitable for this application. The density is increased from 82.4% to 90.1%, and hardness is promoted from 664 to 711 HV, by adding 0.25 mole of Al to the garnet structure whereas it decreased by the addition of a higher amount of Al. It is worth mentioning that hardness is in direct proportion with elastic modulus. As widely known, increasing the elastic modulus leads to higher resistance over Li dendrite formation during cycling. This result reveals that optimum Al content increases the stability of LLZO over Li dendrite formation and short circuits during charge and discharge cycling.

Variations of garnet density concerning the concentrations of Al are given in Fig. 3. This improvement in mechanical and physical properties may be resulted from better sintering due to the increasing intergranular melting and enhancing densification as a result of the addition of Al dopant. The researches have shown that in garnet containing 0.22 mole of Al, shrinkage begins at a temperature of 1055°C, which is related to the liquid phase sintering [15].

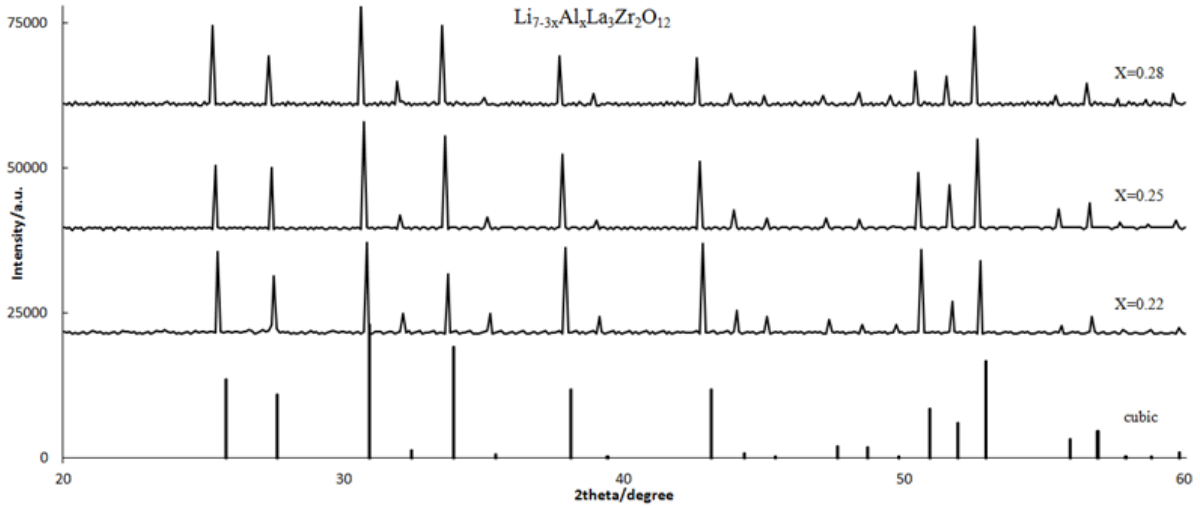

Fig. 2. XRD pattern of garnet samples doped with different amounts of Al, sintered at 1180°C for 10 hours

Table 1. Hardness and Relative density of Al-doped LLZO garnet at 1180°C for 10 hour

Sample	Hardness(HV)	Relative Density (%)
LLZO(X=0.22)	664±10	82.4±0.1
LLZO(X=0.25)	711±10	90.1±0.1
LLZO(X=0.28)	698±10	87.5±0.1

[DOI: 10.22068/ijmse.2631]

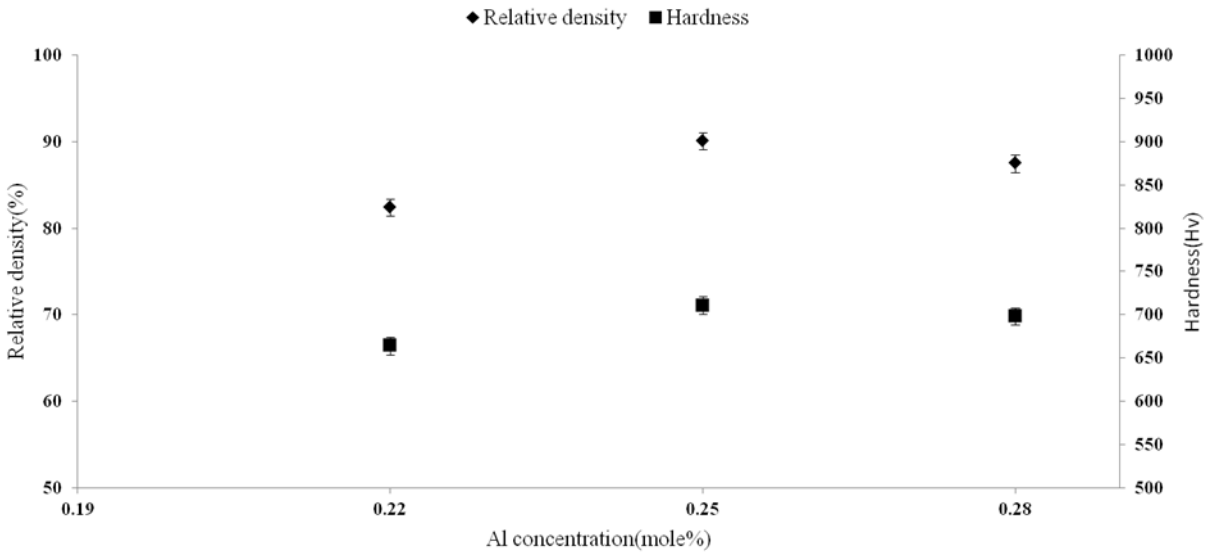

Fig. 3. Variation of hardness and density of sintered Al-doped LLZO garnet with the concentration of Al.

Yang et al. observed that the density of garnet with no additive was 2.36 g cm^{-3}, which increased to 4.4 g cm^{-3} by adding 0.2% by weight of Al and suggested this promotion in density to the presence of liquid phase during sintering [15]. Herein, the higher density by the addition of Al is thought to be due to the promotion of intergranular melting, so the diffusion of Al is enhanced, and the garnet is completely densified. For the sample with 0.28 mol Al, the decrease in density might be due to the segregation of excess Al in grain boundaries. FESEM micrographs (Fig. 4) show that garnet with 0.22 mole of Al revealed that the porosity is following Archimedes density results. Although, the micrographs revealed that the grain size was not affected considerably by the addition of Al. This trend was also evident in density and hardness, and the low density and hardness of this sample confirm this. FESEM micrographs of garnet cross-sections with 0.22, 0.25, and 0.28 moles Al in Fig. 4 are shown. The effect of Al dopant on ionic conductivity and electrochemical properties of LLZO were investigated using EIS. The Nyquist plots of samples with different amounts of Al are presented in Fig. 5. As can be seen, samples with different amounts of Al, a semicircle can be fitted in high frequencies. Although, distinct semicircles are not distinguishable and therefore it is not possible to distinguish the bulk and grain boundaries conductivity. The data values of ionic conductivity are presented in table 2. Typically, the ionic conductivity of polycrystalline ceramic increases with the increase in density especially bulk conductivity [48]. These results revealed that in the sample with 0.25 mole Al which had the highest density, it has the ionic conductivity about 4 times of other samples.

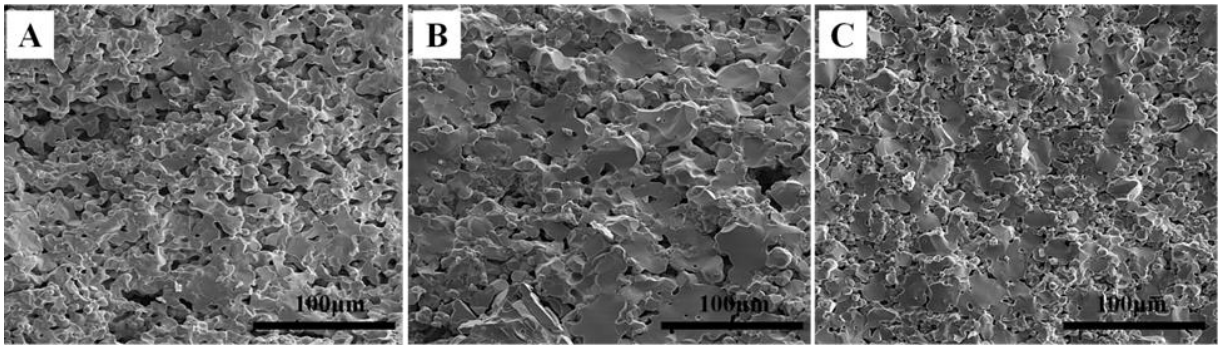

Fig. 4. Field emission scanning electron microscope image of the fracture section, a) 0.22 mole of Al additive b) 0.25 mole of Al additive and c) 0.28 mole of Al additive, sintered at 1180°C for 10 hours.

[DOI: 10.22068/ijmse.2631]

It is worth mentioning that the addition of Al increases the conductivity of the samples by the order of 10 times [11, 33, 47].
Additionally, the excess Al can segregate at the grain boundary and cause an irregular structure at the grain boundary. This behavior seems to increase the activation energy in the sample with 0.28 mole Al and decrease the total conductivity rather than sample relatively high density. Also, Al segregation can affect grain growth by covering the grain boundary. This was seen in the sample with 0.28 mole Al, which could lead to an increase in grain boundary resistivity. In Table 3, the results of other research have been presented. The optimum concentration identified for Al dopant in this study is 0.25 mol. It should be mentioned that the result of this work is higher than the sample synthesized by using the sol-gel and molten salt method. Moreover, the ionic conductivity of the optimum sample is comparable to the result of the solid-state sample. We believe the improved conductivity reported here is might be due to a low level of impurities in the raw material allowing better tuning of the dopant content.

Table 2. Total conductivity (σ_T) for different Al mole dopants at 25°C.

Al-doped content (mole)	σ_T (S. cm^{-1})
0.22	0.94 x 10^{-4}
0.25	4.7 x 10^{-4}
0.28	1.12 x 10^{-4}

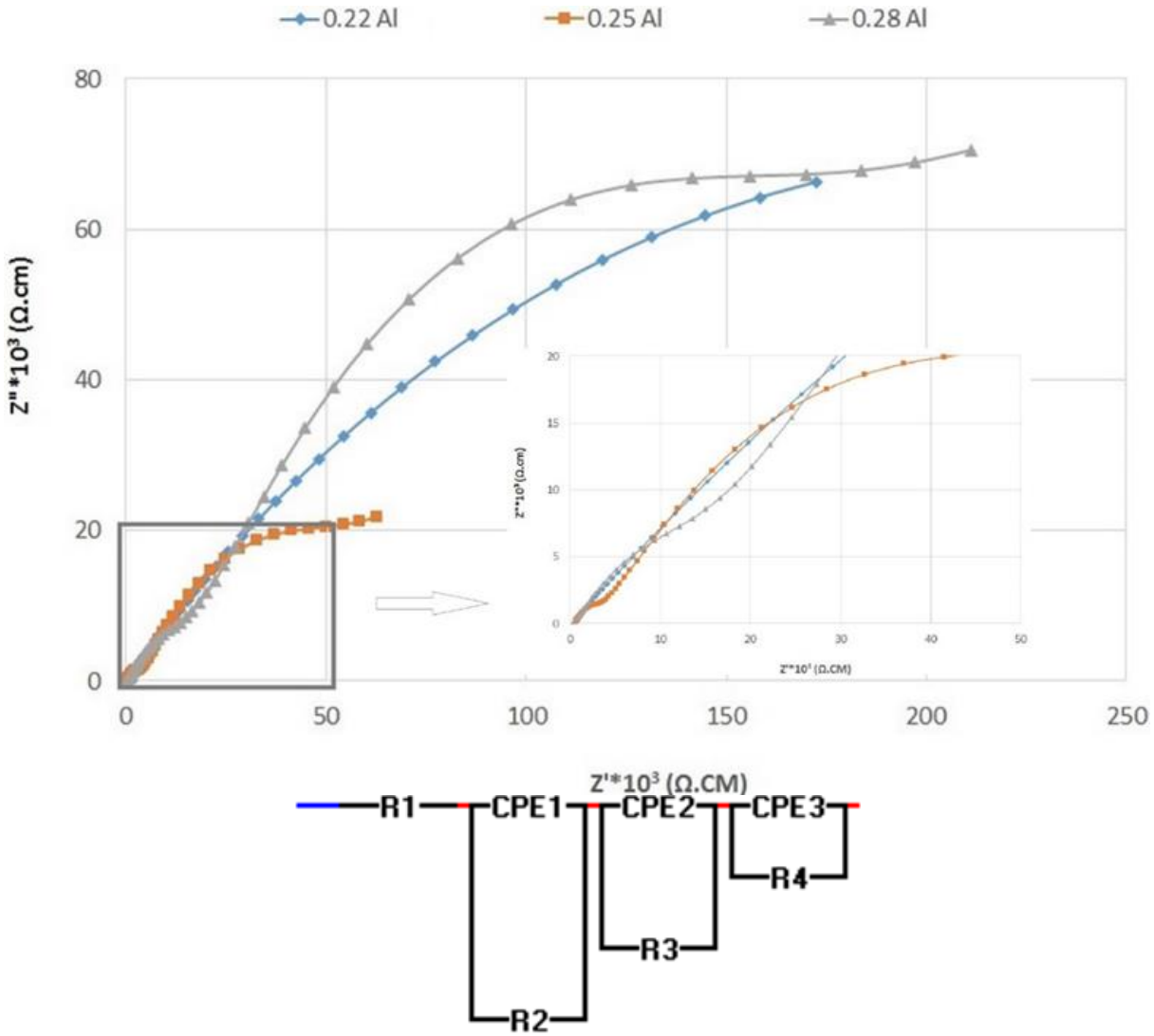

Fig. 5. Impedance image of $Li_{7-3x}Al_xLa_3Zr_2O_{12}$ garnet (x= 0, 0.22, 0.25, and 0.28).

[DOI: 10.22068/ijmse.2631]

Table 3. Literature overview for processing LLZO pellet.

Compound	Synthesis conditions	Dopant	Ionic conductivity ($S.cm^{-1}$)	Relative density	Ref
$Li_{6.16}Al_{0.28}La_3Zr_2O_{12}$	Solid-state	Al (0.28mol)	4.89×10^{-4}	94%	[15]
$Li_{6.6}Al_{0.2}La_3Zr_2O_{12}$	Sol-gel	Al (0.2 mol)	2.4×10^{-6}	88%	[28]
$Li_{6.1}La_3Zr_2Al_{0.25}O_{11.98}$	Molten salt	Al(0.25 mol)	9.13×10^{-6}	85%	[17]
Present work	Sol-gel combustion	Al(0.22 mol) Al(0.25 mol) Al(0.28 mol)	9.4×10^{-5} 4.7×10^{-4} 1.12×10^{-4}	82.5% 91% 87.5%	

4. CONCLUSIONS

In this study, a facile sol-gel combustion method was used to synthesize Al-doped LLZO. The XRD results revealed that the addition of Al dopant promoted the formation of cubic phase by increasing the lithium vacancy concentration and destabilizing lithium in the tetragonal phase. Besides, the addition of 0.28 mole Al resulted in full stabilization of the cubic phase. Although, after sintering as a result of lithium loss and an increase in lithium vacancy concentration, even for the sample with 0.25 mole Al, the cubic phase was fully stabilized. The density study of different samples revealed that Al promoted densification of LLZO samples, whereas the relative density of sample Al-free increased from 76.5 to 82.4% by adding 0.22 mole Al. The latter may be due to the inter-granular melting by the addition of Al. However, the sample with 0.28 mole Al had a lower density, which may be due to the limitation of Al solubility in LLZO structure and the formation of a second phase, not in the XRD detection range. The EIS results revealed that the sample with 0.25 Al-dopant had the highest total conductivity. The addition of Al can be considered as a promising approah in improving the bulk and ionic conductivity. The optimized amount of Al addition seems to be 0.25 mol which increased both the density as well as ionic conductivity.

ACKNOWLEDGMENT

This work is based upon research funded by Iran National Science Foundation (INSF) under project No. 4000823.

REFERENCES

[1] Golmohammad, M., Maleki Shahraki, M., Golestanifard, F, Mirhabibi, A., Yang, G., Synthesis and characterization of nanoflaky maghemite (γ-Fe_2O_3) as a versatile anode for Li-ion batteries. Ceramics International, 2019. 45(1), 131-136.

[2] Golmohammad, M., Mirhabibi, A., Golestanifard, F., Erik, K., Optimizing Synthesis of Maghemite Nanoparticles as an Anode for Li-Ion Batteries by Exploiting Design of Experiment. Journal of Electronic Materials, 2016. 45(1), 426-434.

[3] Golmohammad, M., Golestanifard, F., Mirhabibi, A., Kelder, E., Synthesis and characterization of porous maghemite as an anode for Li-ion batteries. Ceramics International, 2016. 42(3), 4370-4376.

[4] Golmohammad, M., Golestanifard, F., and Mirhabibi, A., Synthesis and Characterization of Maghemite as an Anode for Lithium-Ion Batteries. International Journal of Electrochemical Science, 2016. 11, 6432-6442.

[5] Larraz, G., Orera, A., and Sanjuán, M.L., Cubic phases of garnet-type $Li_7La_3Zr_2O_{12}$: the role of hydration. Journal of Materials Chemistry A, 2013. 1(37), 11419-11428.

[6] Tsai, C.-L., Dashjav, E., Hammer, E. Finsterbusch, M., Tietz, F., Uhlenbruck, S., High conductivity of mixed phase Al-substituted $Li_7La_3Zr_2O_{12}$. Journal of Electroceramics, 2015. 35(1), 25-32.

[7] Murugan, R., Thangadurai, V., and Weppner, W., Fast Lithium Ion Conduction in Garnet-Type $Li_7La_3Zr_2O_{12}$. Angewandte Chemie International Edition, 2007. 46(41), 7778-7781.

[8] Zheng, F., Kotobuki, M., Song, S.m Lai, M., Lu, L., Review on solid electrolytes for all-solid-state lithium-ion batteries. Journal of Power Sources, 2018. 389, 198-213.

[9] Janani, N, Deviannapoorani, C., Dhivyaa, L., Murugan, R., Influence of sintering

[DOI: 10.22068/ijmse.2631]

additives on densification and Li^+ conductivity of Al doped $Li_7La_3Zr_2O_{12}$ lithium garnet. RSC Advances, 2014. 4(93), 51228-51238.

[10] Huang, M., Liu, T., Deng, Y., Geng, H., Shen, Y., Lin, Y., Nan, C., Effect of sintering temperature on structure and ionic conductivity of $Li_{7-x}La_3Zr_2O_{12-0.5x}$ (x= 0.5~0.7) ceramics. Solid State Ionics, 2011. 204-205, 41-45.

[11] Chen, R.-J., Huang, M., Huang, W. -Z, Shen, Y., Lin, Y., Nan, C., Effect of calcining and Al doping on structure and conductivity of $Li_7La_3Zr_2O_{12}$. Solid State Ionics, 2014. 265, 7-12

[12] Bachman, J., Muy, S., Grimaud, A., Chang, H., Pour, N., Lux, S., Paschos, O., Maglia, F., Lupart, S., Lamp, P., Giordano, L., Horn, Y., Inorganic solid-state electrolytes for lithium batteries: mechanisms and properties governing ion conduction. Chemical reviews, 2015. 116(1), 140-162.

[13] Rosenkiewitz, N., Schumacher, J., Bockmeyer, M., Deubener, J., Nitrogen-free sol–gel synthesis of Al-substituted cubic garnet $Li_7La_3Zr_2O_{12}$ (LLZO). Journal of Power Sources, 2015. 278, 104-108.

[14] Badami, P., Smetaczek, S., Limbeck, A., Rettenwander, D., Chan, C., Nadar Mada Kannan, N., Facile synthesis of Al-stabilized lithium garnets by a solution-combustion technique for all solid-state batteries. Materials Advances, 2021. 2(15), 5181-5188.

[15] Yang, T., Li, Y., Wu, W., Cao, Z., He, W., Gao, Y., Liu, J., Li, G., The synergistic effect of dual substitution of Al and Sb on structure and ionic conductivity of $Li_7La_3Zr_2O_{12}$ ceramic. Ceramics International, 2018. 44(2), 1538-1544.

[16] Ashuri, M., Golmohammad, M., Soleimany Mehranjani, A., Faghihi Sani, M, Al-doped $Li_7La_3Zr_2O_{12}$ garnet-type solid electrolytes for solid-state Li-Ion batteries. Journal of Materials Science: Materials in Electronics, 2021. 32(5), 6369-6378.

[17] Zhang, Y., Liu, A., Shi, Z., Ge, S., Zhang, J., Microstructure and ion conductivity of Al-LLZO solid electrolyte prepared by molten salt and cold sintering process. International Journal of Applied Ceramic Technology, 2022. 19, 320-331.

[18] Wu, J.-F., Chen, E., Yi, Y., Liu, L. Pang, W., Peterson, V., Guo, X., Gallium-Doped Li7La3Zr2O12 Garnet-Type Electrolytes with High Lithium-Ion Conductivity. ACS Applied Materials & Interfaces, 2017. 9(2), 1542-1552.

[19] Li, C., Liu, Y., He, J., Brinkman, K., Ga-substituted Li7La3Zr2O12: An investigation based on grain coarsening in garnet-type lithium ion conductors. Journal of Alloys and Compounds, 2017. 695, 3744-3752.

[20] Howard, M., Clemens, O, Kendrick, E., Knight, K. S., Slater, P. R.,, Effect of Ga incorporation on the structure and Li ion conductivity of $La_3Zr_2Li_7O_{12}$. Dalton Transactions, 2012. 41(39), 12048-12053.

[21] Jalem, R., Rushton, M., Manalastas, W., Kilner, J., Grimes, R., Effects of Gallium Doping in Garnet-Type $Li_7La_3Zr_2O_{12}$ Solid Electrolytes. Chemistry of Materials, 2015. 27(8), 2821-2831.

[22] Huang, M., Shoji, M., Shen, Y., Nan, C. W., Munakata, H., Kanamura, K., Preparation and electrochemical properties of Zr-site substituted $Li_7La_3(Zr_{2-x}M_x)O_{12}$ (M= Ta, Nb) solid electrolytes. Journal of Power Sources, 2014. 261, 206-211.

[23] Lee, H.C., Oh, N. R., Yoo, A. R., Kim, Y., Sakamoto, J., Preparation of a $Li_7La_3Zr_{1.5}Nb_{0.5}O_{12}$ Garnet Solid Electrolyte Ceramic by using Sol-gel Powder Synthesis and Hot Pressing and Its Characterization. Journal of the Korean Physical Society, 2018. 73(10), 1535-1540.

[24] Yoon, S.A., Oh, N. R., Yoo, A. R., Lee, H. G., Lee, H. C., Preparation and Characterization of Ta-substituted $Li_7La_3Zr_{2-x}O_{12}$ Garnet Solid Electrolyte by Sol-Gel Processing. J. Korean Ceram. Soc, 2017. 54(4), 278-284.

[25] Dhivya, L., and Murugan, R., Effect of simultaneous substitution of Y and Ta on the stabilization of cubic phase, microstructure, and Li^+ conductivity of $Li_7La_3Zr_2O_{12}$ lithium garnet. ACS applied materials & interfaces, 2014. 6(20), 17606-17615.

[26] Zhang, Y., Deng, J., Hu, D., Chen, F., Shen, Q., Dong, S., Synergistic regulation

[DOI: 10.22068/ijmse.2631]

of garnet-type Ta-doped $Li_7La_3Zr_2O_{12}$ solid electrolyte by Li_+ concentration and Li_+ transport channel size. Electrochimica Acta, 2019. 296, 823-829.

[27] Matsuda, Y., Sakamoto, K., Matsui, M., Yamamoto, O., Takeda, Y., Imanishi, N., Phase formation of a garnet-type lithium-ion conductor $Li_{7-3x}Al_xLa_3Zr_2O_{12}$. Solid State Ionics, 2015. 277, 23-29.

[28] Rangasamy, E., Wolfenstine, J., Allen, J., Sakamoto, J., The effect of 24c-site (A) cation substitution on the tetragonal–cubic phase transition in $Li_{7-x}La_{3-x}A_xZr_2O_{12}$ garnet-based ceramic electrolyte. Journal of Power Sources, 2013. 230, 261-266.

[29] Im, C., Park, D., Kim, H., Lee, J., Al-incorporation into $Li_7La_3Zr_2O_{12}$ solid electrolyte keeping stabilized cubic phase for all-solid-state Li batteries. Journal of Energy Chemistry, 2018. 27(5), 1501-1508.

[30] Li, Y., Han, J. –T., Wang, C. –A, Vogel, S., Xie, H., Xu, M., Goodenough, J., Ionic distribution and conductivity in lithium garnet $Li_7La_3Zr_2O_{12}$. Journal of Power Sources, 2012. 209, 278-281.

[31] Gordon, Z.D., Yang, T., Morgado, G., Chan, C., Preparation of Nano- and Microstructured Garnet $Li_7La_3Zr_2O_{12}$ Solid Electrolytes for Li-Ion Batteries via Cellulose Templating. ACS Sustainable Chemistry & Engineering, 2016. 4(12), 6391-6398.

[32] Bitzer, M., T. Van Gestel, and S. Uhlenbruck, Sol-gel synthesis of thin solid $Li_7La_3Zr_2O_{12}$ electrolyte films for Li-ion batteries. Thin Solid Films, 2016. 615, 128-134.

[33] Kokal, I., Somer, M., Notten, P. H. L., Hintzen, H. T., Sol–gel synthesis and lithium ion conductivity of $Li_7La_3Zr_2O_{12}$ with garnet-related type structure. Solid State Ionics, 2011. 185(1), 42-46.

[34] Awaka, J., Kijima, N., Hayakawa, H., Akimoto, J., Synthesis and structure analysis of tetragonal $Li_7La_3Zr_2O_{12}$ with the garnet-related type structure. Journal of Solid State Chemistry, 2009. 182(8), 2046-2052.

[35] Cheng, L., Park, J., Hou, H., Zorba, V., Chen, G., Richardson, T., Cabana, J., Russo, R., Doeff, M., Effect of microstructure and surface impurity segregation on the electrical and electrochemical properties of dense Al-substituted $Li_7La_3Zr_2O_{12}$. Journal of Materials Chemistry A, 2014. 2(1), 172-181.

[36] Allen, J.L., Wolfenstine, J., Rangasamy, E., Sakamoto, J., Effect of substitution (Ta, Al, Ga) on the conductivity of $Li_7La_3Zr_2O_{12}$. Journal of Power Sources, 2012. 206, 315-319.

[37] Tan, J.J., Tiwari, A., Synthesis of Cubic Phase $Li_7La_3Zr_2O_{12}$ Electrolyte for Solid-State Lithium-Ion Batteries. Electrochemical and Solid State Letters, 2012. 15(3), A37-A39.

[38] Yoo, A.R., Yoon, S., Yun, K., Sakamoto, J., Lee, H., A Comparative Study on the Synthesis of Al-Doped $Li_{6.2}La_3Zr_2O_{12}$ Powder as a Solid Electrolyte Using Sol-Gel Synthesis and Solid-State Processing. Journal of Nanoscience and Nanotechnology, 2016. 16(11), 11662-11668.

[39] Djenadic, R., Botros, M., Benel, C., Clemens, O., Bergfeldt, T., Hahn, H., Nebulized spray pyrolysis of Al-doped $Li_7La_3Zr_2O_{12}$ solid electrolyte for battery applications. Solid State Ionics, 2014. 263, 49-56.

[40] Bai, L., Xue, W., Li, Y., Liu, X., Li, Y., Sun, J., The surface behaviour of an Al-$Li_7La_3Zr_2O_{12}$ solid electrolyte. Ceramics International, 2017. 43(17), 15805-15810.

[41] Takano, R., Tadanaga, K., Hayashi, A., Tatsumisago, M., Low temperature synthesis of Al-doped $Li_7La_3Zr_2O_{12}$ solid electrolyte by a sol–gel process. Solid State Ionics, 2014. 255, 104-107.

[42] Sudreau, F., D. Petit, and J.P. Boilot, Dimorphism, phase transitions, and transport properties in $LiZr_2(PO_4)_3$. Journal of Solid State Chemistry, 1989. 83(1), 78-90.

[43] Aono, H., Sugimoto, E., Sadaoka, Y., Imanaka, N., Adachi, G., Ionic conductivity and sinterability of lithium titanium phosphate system. Solid State Ionics, 1990. 40-41, 38-42.

[44] Hubaud, A.A., Schroeder, D., Key, B., Ingram, B., Doga, F., Vaughey, J., Low temperature stabilization of cubic

[DOI: 10.22068/ijmse.2631]

($Li_{7-x}Al_{x/3}$) $La_3Zr_2O_{12}$: role of aluminum during formation. Journal of Materials Chemistry A, 2013. 1(31), 8813-8818.

[45] Matsui, M., Takahashi, K., Sakamoto, K., Hirano, A., Takeda, Y., Yamamoto, O., Imanishi, N., Phase stability of a garnet-type lithium ion conductor $Li_7La_3Zr_2O_{12}$. Dalton Transactions, 2014. 43(3), 1019-1024.

[46] Geiger, C.A., Alekseev, E., Lazic, B., Fisch, M., Armbruster, T., Langer, R., Fechtelkord, M., Kim, N., Pettke, T., Weppner, W., Crystal chemistry and stability of "$Li_7La_3Zr_2O_{12}$" garnet: a fast lithium-ion conductor. Inorganic chemistry, 2010. 50(3), 1089-1097.

[47] Kamaya, N., Homma, K., Yamakawa, Y., Hirayama, M., Kanno, R., Kato, Y., Hama, S., Kawamoto, K., Mitsui, A., A lithium superionic conductor. Nature Materials, 2011. 10, 682.

[48] West, W., J. Whitacre, J., and Lim, J., Chemical stability enhancement of lithium conducting solid electrolyte plates using sputtered LiPON thin films. Journal of power sources, 2004. 126(1-2), 134-138.

[DOI: 10.22068/ijmse.2631]